

A Unified Framework for Modality-Agnostic Deepfakes Detection

Cai Yu, Peng Chen, Jiahe Tian, Jin Liu, Jiao Dai, Xi Wang, Yesheng Chai, Shan Jia, Siwei Lyu, *Fellow, IEEE*, Jizhong Han, *Member, IEEE*

Abstract—As AI-generated content (AIGC) thrives, deepfakes have expanded from single-modality falsification to cross-modal fake content creation, where either audio or visual components can be manipulated. While using two unimodal detectors can detect audio-visual deepfakes, cross-modal forgery clues could be overlooked. Existing multimodal deepfake detection methods typically establish correspondence between the audio and visual modalities for binary real/fake classification, and require the co-occurrence of both modalities. However, in real-world multi-modal applications, missing modality scenarios may occur where either modality is unavailable. In such cases, audio-visual detection methods are less practical than two independent unimodal methods. Consequently, the detector can not always obtain the number or type of manipulated modalities beforehand, necessitating a fake-modality-agnostic audio-visual detector. In this work, we introduce a comprehensive framework that is agnostic to fake modalities, which facilitates the identification of multimodal deepfakes and handles situations with missing modalities, regardless of the manipulations embedded in audio, video, or even cross-modal forms. To enhance the modeling of cross-modal forgery clues, we employ audio-visual speech recognition (AVSR) as a preliminary task. This efficiently extracts speech correlations across modalities, a feature challenging for deepfakes to replicate. Additionally, we propose a dual-label detection approach that follows the structure of AVSR to support the independent detection of each modality. Extensive experiments on three audio-visual datasets show that our scheme outperforms state-of-the-art detection methods with promising performance on modality-agnostic audio/video deepfakes.

Index Terms—Multimedia forensics, Multimodal learning, Video Forgery detection.

I. INTRODUCTION

AS artificial intelligence-generated content (AIGC) technologies continue to advance, deepfakes are evolving to become increasingly complex and diverse in form.

Traditional deepfakes mainly generate fake faces or voices tied to a specific person within a single modality, either through visual deepfake generation techniques [1–3] or audio synthesis methods [4, 5]. For instance, a deepfake video falsely depicting New Zealand Prime Minister Jacinda Ardern

C. Yu, J. Tian, and J. Liu are with the Institute of Information Engineering, Chinese Academy of Sciences, Beijing, China, and also with the School of Cyber Security, University of Chinese Academy of Sciences, Beijing, China. E-mail: (caiyu, tianjiahe, liujin)@iie.ac.cn.

P. Chen is with the RealAI Inc, Beijing, China. E-mail: peng.chen@realai.ai.

J. Dai, X. Wang, Y. Chai, and J. Han are with the Institute of Information Engineering, Chinese Academy of Sciences, Beijing, China. E-mail: (daijiao, wangx1, chaiyesheng, hanjizhong)@iie.ac.cn.

S. Jia, and S. Lyu are with the Department of Computer Science and Engineering, University at Buffalo, State University of New York, NY, USA. E-mail: (shanjia, siweilyu)@buffalo.edu.

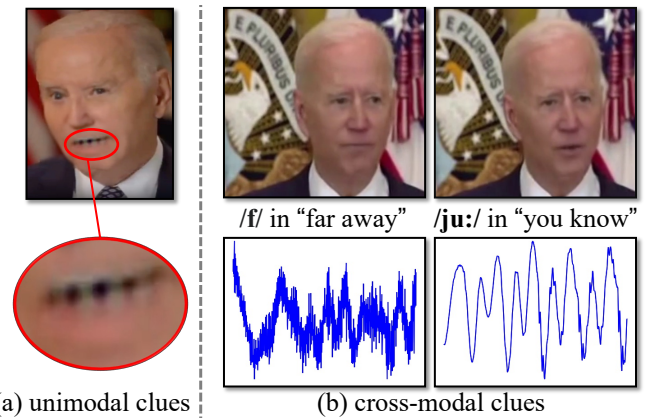


Fig. 1: Forgery patterns in deepfakes³. (a) Visual artifacts within a single modality: Biden’s teeth exhibit an irregular shape. (b) Cross-modal speech mismatch in deepfakes. The phoneme-level audio waveform corresponds to the duration of the frame shown above. Both images reveal a speech mismatch between lip motions and audio sounds. On the left, Biden’s mouth is in a closed state before pronouncing the “f” sound and has not yet produced a complete syllable. However, the audio image displays a complex frequency wave that should only appear during active pronunciation. On the right, Biden is uttering the vowels in “you”, but the sound waves show rather simple frequency patterns, which are typically indicative of panting or background noise rather than speech.

smoking crack cocaine circulated widely on social media¹. In another example, AI-generated audio mimicking Donald Trump was used to scam Trump voters². These instances underscore the growing sophistication and potential impact of deepfake technologies. However, the landscape of deepfake technology is rapidly evolving. Cutting-edge deepfake methods like Wav2Lip [6] and VideoReTalking [7] can even achieve cross-modal forgery by driving audio to generate precise lip-sync videos. To date, malicious attackers have already been capable of combining the above technologies to create multimodal forgeries in which both the face and voice of the target individual can be seamlessly manipulated. As video examples in Figure 1 show, the fake ‘Biden’ in these videos is uttering nonsense in a voice that exactly mimics his

¹<https://www.youtube.com/shorts/j0v4UMnHn1M>

²<https://www.tiktok.com/t/ZT8MWGQ4g/>

³videos of these examples are cited from <https://deepfakes.lol/>, and <https://www.tiktok.com/t/ZT8M7GmQg/>

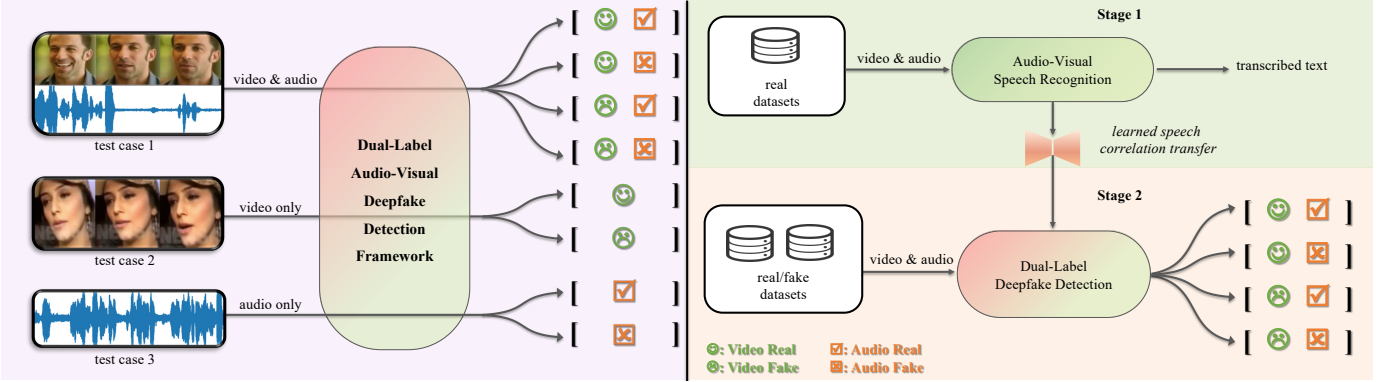


Fig. 2: Modality-Agnostic Audio-Visual Deepfake Detection: The figure on the left shows three modality-agnostic detection scenarios that our detector supports. This detector enables independent detection of forgery in each modality and can handle scenarios where either modality is unavailable. The figure on the right illustrates the general scheme of our method, which leverages the speech correlation across modalities via the AVSR task to perform dual-label detection.

own. Compared to unimodal deepfakes, multimodal deepfakes, owing to their multi-faceted forgeries, could be more realistic and thus much harder to discern.

Consequently, deepfakes have evolved to include not only audio and visual but also cross-modal forms, thereby exacerbating their detrimental impact accordingly. This evolution raises new challenges for detection methods, making the fight against deepfakes even more complex: Deepfake content can now appear in various forms across social media (audio-only, video-only, or audio-visual pairs), and a single detector may not always have access to the range or type of manipulated modalities beforehand. While employing two separate unimodal detectors seems like a viable approach, the cross-modal forgery clues generated might be overlooked. The comparison in Figure 1 shows that the fake frames in (b) do not exhibit visual artifacts as obvious as those in (a). Yet, when paired with audio, these frames reveal a phoneme-level mismatch in speech. This observation implies that when no readily apparent forgery patterns are detectable within a single modality, employing a cross-modal detector could be more effective in capturing forgery patterns across multiple modalities. Considering the significance of multimedia content security, it is crucial to develop a unified, multimodal framework that can effectively defend against emerging deepfakes, irrespective of the number or type of modalities involved.

Nowadays, a few emerging audio-visual deepfake detection methods [8–10] have achieved promising results. For example, EmoForen [10] detects deepfakes via emotional inconsistency. These methods typically treat audio as a reference signal to assess the level of audio-visual consistency, ultimately generating a single binary real/fake label for the entire video.

More recent methods, such as JointAV [11] and AVoiD-DF [12], attempt to leverage cross-attention to learn potential cross-modal dependence. However, more effective perceptual cues remain underutilized. Besides, all the abovementioned methods necessitate the presence of audio and video in pairs. However, in the real world, deepfakes do not always appear in audio-visual pairs. There are detection scenarios where either the audio or visual component of the media is missing

or unavailable. In such modality-agnostic situations, relying solely on audio-visual detection methods may be less practical than employing two separate unimodal detection methods. Nevertheless, audio-visual detection remains vital for identifying cross-modal forgery clues. This raises a critical question: Is there a “best of both worlds” approach for an audio-visual detection framework that can effectively leverage cross-modal forgery clues while still maintaining robust performance in modality-agnostic scenarios?

In this work, we propose a unified framework for audio-visual deepfake detection that targets modality-agnostic scenarios. First, to effectively capture cross-modal forgery clues, we introduce Audio-Visual Speech Recognition (AVSR) as a preliminary task (as illustrated on the right of Figure 2). This practice is motivated by the observation that natural phonation processes exhibit consistent dynamic patterns between audio and visual modalities. Conversely, such subtle, speech-related correlations may be challenging for deepfakes to replicate due to their unnatural origins. By pretraining on a large number of real videos, the AVSR model learns to map both audio and visual signals to the same set of spoken characters. This makes it well-suited for extracting natural speech correlations across modalities. By transferring this speech correlation into our framework, the modeling of cross-modal forgery clues can be enhanced. Customized for deepfake detection, a Modality Compensation Adapter is inserted into the AVSR model to alleviate modality imbalance in model decisions. Second, to support the independent detection of each modality, we propose a dual-label detection approach where independent labels are assigned for each modality so that even if one modality is missing, the detection of the other will not be affected (as illustrated on the left of Figure 2). Based on this insight, a Dual-Label Classifier is designed and established with a Fake Composition Detector to extract forgery intensity and a Temporal Aggregation Module to capture temporal inconsistency. The Dual-Label detection approach establishes a parallel structure between each modality, which aligns with the AVSR structure, thereby maximizing AVSR’s advantages. The unified structure formed by the combination of AVSR

TABLE I: Comparison of various audio-visual deepfake detection methods. Methods are evaluated based on the approach of modeling cross-modal forgery patterns (Forgery Pattern Modeling), the type of classification approach used (Classification Approach), their capability to specify which modality has been manipulated (Forgery Modality Identification), and whether they can detect modality-agnostic deepfakes when a modality is missing (Support for Missing Modality).

Methods	Year	Forgery Pattern Modeling	Classification Approach	Forgery Modality Identification	Support for Missing Modality
MDS [8]	2020	Modality Dissonance Score	Binary	×	×
EmoForen [10]	2020	Emotion Consistency	Binary	×	×
JointAV [11]	2021	Inter-modal Attention	Triple-Classifier	✓	×
VFD [13]	2022	Identity Similarity	Binary	×	×
RealForensics [14]	2022	Cross-modal Self-supervised Learning	Binary	×	×
BA-TFD [15]	2022	Temporal Synchronization	Binary	×	×
AVoiD-DF [12]	2023	Multi-modal Joint-decoder	Binary	×	×
AVFakeNet [16]	2023	Swin Transformer	Dual-Classifier	✓	×
AVAD [17]	2023	Autoregressive Synchronization	Binary	×	×
PVASS [18]	2023	Self-supervised Visual-audio Alignment	Binary	×	×
Ours	2023	Speech Correlation	Dual-Label	✓	✓

and Dual-Label Classifier guarantees the ability to effectively combat modality-agnostic deepfakes. The contributions of this work are summarized as follows:

- We propose a unified audio-visual deepfake detection framework, incorporating AVSR as a preliminary task to model cross-modality correlation. Tailored for multi-modal deepfake detection, we design a Modality Compensation Adapter within the AVSR architecture to effectively balance the visual and audio modalities.
- We advocate for a modality-agnostic approach to handle various deepfakes and reformulate audio-visual deepfake detection into a dual-label framework. A Dual-Label Classifier is developed to independently predict the authenticity of each modality. A Temporal Aggregation Module and a Fake Composition Detector are further integrated to enhance the classifier. To the best of our knowledge, this is the first work to enable detection of both multi-modal and single modality deepfakes.
- Extensive experiments on three datasets demonstrate the superiority and flexibility of our framework in detecting modality-agnostic deepfakes.

II. RELATED WORK

Extensive research has been dedicated to detecting deepfakes in multimedia content. According to the modality involved, methods for deepfake detection can be broadly divided into three categories as follows.

A. Visual Modality Deepfake Detection

These methods perform image-level or video-level real/fake prediction. Image-level methods focus on image or intra-frame artifacts. Face X-ray [19] and SBIs [20] target forgery artifacts of blending boundaries by simulating deepfake images. PEL [21], PADD [22], and MaDD [23] exploit fine-grained clues to detect face forgery. As to video-level methods, previous works leverage biometric signals to detect deepfake videos, such as facial action patterns [24, 25] and eye blinking [26]. Another branch of video-level works utilizes temporal modeling [27–29] for classification since manipulation in fake videos usually causes temporal inconsistency. Arguing that the above tangible

clues may make models overfit to low-level manipulation-specific artifacts, LipForens [30] proposes to catch high-level semantic inconsistency via a lipreading network. Regarding the utilization of high-level information, LipForens is highly relevant to our work. However, unlike our proposal, the utility of audio has been neglected.

B. Auditory Modality Deepfake Detection

Audio deepfake detection mainly counters the voice spoofing synthesized by texts-to-speech (TTS) or voice conversion (VC) techniques. Some works [31–33] apply pretrained speech representation models, such as wav2vec2 [34], to detect spoofed audio. Other works leverage classic speech tasks to improve audio deepfake detection; for example, DAD-SV [35] boils down deepfake detection into a speaker verification problem. These works also render a high plausibility for us to introduce speech recognition to detect multimodal deepfakes.

C. Audio-Visual Deepfake Detection

There exist a few methods involving both visual and auditory modalities. However, most of them intrinsically measure the degree of audio-visual correspondence [8, 10, 36] or treat audio signals as reference [14] for video so that they can only assign a binary real/fake label for the entire video. For example, MDS [8] measures the audio-visual dissonance in a video via the Modality Dissonance Score. EmoForen [10] leverage emotion clues to discern fake videos. Nevertheless, these methods can only determine whether audio and visual components are consistent or not; they cannot specifically predict which modality has been manipulated. JointAV [11] and AVFakeNet [16] have attempted to detect manipulation in each modality using a multi-classifier approach. However, they primarily rely on the attention mechanism to capture cross-modal dependencies of the audio-visual pairs, while the high-level perceptual information such as speech correlation is underutilized. Moreover, none of the aforementioned methods have discussed how their multimodal detectors perform when encountering scenarios with missing modalities. For a detailed comparison of current audio-visual deepfake detection methods, refer to Table I.

III. HOW AVSR BENEFITS DEEPFAKE DETECTION

In this section, we aim to provide a comprehensive explanation of our motivation behind introducing AVSR as the preliminary task, focusing specifically on two aspects.

A. Biological Perspective

Human perception of speech involves both audition and vision. The cortical correlates of seen speech suggest that auditory processing of speech is affected by vision at both neurological and perceptual levels [37]. Biological studies have shown that for speech perception, the visual channel and auditory channel share similar dynamic patterns [38]. Thus, we seek to leverage this kind of high-level audio-visual correlation, or, more precisely, audio-visual speech correlation [39], to identify real/fake audio-visual media. The rationale is that the correlation between audio and visual speech features is an intrinsic characteristic of the natural phonation process, which can be absent in deepfake videos due to the artificial synthesis process. In deepfakes, the visual and audio components are typically initially separated, allowing either of them to be synthesized individually before being merged together. This will inevitably lead to abnormal audio-visual correlations. A study by [40] has identified phoneme-viseme mismatches in deepfakes when “M”, “B”, and “P” are pronounced. Our observations in Figure 1 (b) reveal a similar disruption in speech correlation across modalities. As the feature quality of audio-visual correlation can be reflected by AVSR [39], we choose it as the preliminary task in our framework to enhance the modeling of cross-modal forgery clues.

B. Applications Perspective

In real-world multimodal applications, it is common to encounter situations where either the audio or visual component is missing or unavailable [41]. This also applies to the field of audio-visual deepfake detection. For our framework, we aim to strike a balance in cross-modal dependencies—sufficiently strong to mutually enhance the detection of each modality, yet not overly strong as to compromise performance when a specific modality is missing. The application scenario of AVSR aligns well with this objective, offering a moderate level of cross-modal dependency. Before the advent of AVSR, both ASR (Audio Speech Recognition) [34] and VSR (Visual Speech Recognition) [42] have already exhibited effective performance. The significance of AVSR primarily lies in its ability to compensate for the limitations of these two tasks, such as learning more robust speech representations by leveraging visual signals in noisy speech environments or using speech signals to assist lip-reading models when mouth shapes look similar (e.g., differentiating “b” and “p” phoneme could be better with audio signal combined [43]). Some existing AVSR works have also demonstrated the ability to perform signal-to-character mapping within each modality independently, even when the other modality is absent [44, 45]. This suggests that the cross-modal speech-related dependency in AVSR not only improves speech recognition in each unimodal model but also maintains semantic integrity within each modality when one

is missing. This makes AVSR well-suited for detecting audio-visual deepfakes in complex scenarios, aligning it closely with our modality-agnostic objectives.

IV. METHOD

Given that the probability of forgery for each modality in a video is independent, and either modality may or may not be present, we contend that traditional binary classification methods are not ideal and fall short in handling modality-agnostic scenarios. Our goal is to holistically identify any forged modalities in a video, irrespective of their number or type. To address this, we formulate the deepfake detection task as a dual-label detection approach. This approach is designed to concurrently and independently predict the authenticity of both modalities within a single task. The proposed framework consists of two stages. At the first stage, an encoder-decoder architecture is pretrained on the task of AVSR to extract desired speech correlation. The second stage performs deepfake detection based on acquired speech knowledge. A detailed description of the proposed framework is illustrated in the following subsections.

A. Stage 1: Audio-Visual Speech Recognition

Given a speech recognition dataset $D_{sr} = \{a_t^i, v_t^i, y_t^i\}_{i=1}^{N_{sr}}$ of size N_{sr} , where $t = 1, \dots, T$ denotes time step of input sequence length and a_t^i, v_t^i are the corresponding audio segment and video frame of each time step. For speech recognition task, each time step contains a ground-truth label (word or character) y_t^i . In the setting of this framework, the network produces frame-wise character probabilities $\tilde{y}_t^i \in \{1, \dots, C\}$, where C is the character class. In our implementation, the set $\tilde{y}_t^i \in \{1, \dots, C\}$ consists of 40 phoneme characters.

Speech recognition is a sequence model, which comprises two unimodal encoders θ_a, θ_v , a joint decoder θ_j and a multi-class classifier θ_c . It first extracts unimodal embedding through each encoder, referred to as, $e_t^a = \theta_a(a_t), e_t^v = \theta_v(v_t)$. The final character prediction is obtained by passing the concatenation of two modal embeddings through the decoder and the classifier: $\tilde{y}_t = \theta_c(\theta_j(e_t^a, e_t^v))$. Following [43], the speech recognition network is trained with CTC (Connectionist Temporal Classification) loss [46],

$$\frac{1}{N_{sr}} \sum_{i=1}^{N_{sr}} \mathcal{L}_{CTC}(\tilde{y}_t^i, y_t^i; \theta_a, \theta_v, \theta_j, \theta_c) \quad (1)$$

B. Stage 2: Audio-Visual Deepfake Detection

The process of dual-label deepfake detection is illustrated in Figure 3a. The weights of encoders and the decoder are transferred from that $(\theta_a, \theta_v, \theta_j)$ of speech recognition. A specially designed Modality Compensation Adapter θ_m is inserted into the encoder-decoder and trained from scratch. To perform dual-label detection, we design a dual-label classifier at the end of the network. The design of each component is further detailed in the subsequent subsection.

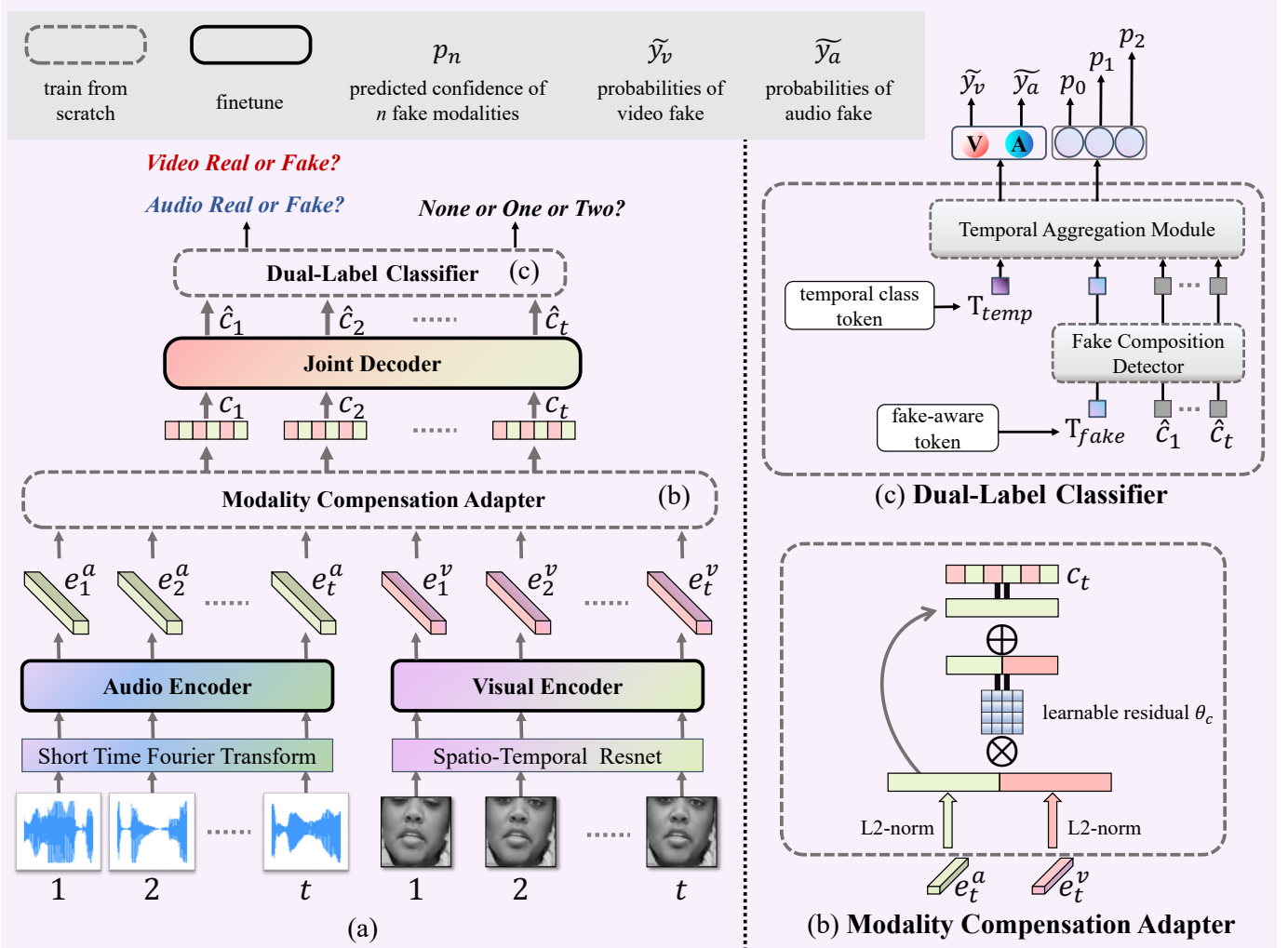


Fig. 3: Demonstration of learning scheme of dual-label deepfake detection. (a) the overview of the proposed framework. The two encoders and joint decoder, which are pretrained on AVSR, are finetuned to model speech correlation across modalities. (b) Modality Compensation Adapter (MCA) is embedded into the encoder-decoder to prevent the network’s over-reliance on a certain modality. (c) Dual-Label Classifier (DLC) is attached at the backend of the model to perform both audio and visual manipulation detection at once.

1) **Problem Formulation:** Given a deepfake detection dataset $D_{df} = \{a_t^j, v_t^j, y_m^j\}_{j=1}^{N_{df}}$, where $y_m \in \{0, 1\}$ is a time-independent label for the entire video, and $m \in \{a, v\}$ denotes the modality dimension (*i.e.*, audio a or video v), the goal of our framework is to predict the y_m^j based on the input a_t^j and/or v_t^j . Compared with a conventional binary prediction for the entire video, where $y^i = 0$ for real or $y^i = 1$ for fake, the dual-label is reflected in that each dimension of the label specifies the possibility of whether each modality has been forged. For example, $y^i = [0, 1]$ denotes the audio is real and video is fake, and $y^i = [1, 1]$ denotes that both audio and video are fake.

2) **Modality Compensation Adapter:** This module is specifically designed for the characteristics of multimodal deepfake detection, aiming at enhancing the adaptability of pre-learned speech correlations to our task. As demonstrated in the recent speech recognition literature, AVSR models can relate audio modality to lexical prediction more effortlessly

than the visual modality [37, 43, 47]. This might cause the audio modality to dominate the model decisions. In terms of deepfake detection, we believe that the differences between reals and fakes may vary across modalities, which could also lead to the model becoming overly reliant on a specific modality. To verify if there is a modality dominance issue in our task, we perform an exploratory baseline experiment of dual-label deepfake detection on randomly sampled videos from the DFDC dataset [48].

TABLE II: An exploratory experiment on detection of each modality in dual-label manner.

	Recall	F1
Visual	76.92	77.39
Audio	57.81	71.49

As shown in Table II, the performance of audio detection is significantly worse than that of video detection. Hence, it is reasonable to speculate that there appears to be some level of

visual dominance in the model decisions. One potential reason is that visual data is much richer than audio data in amount and diversity. Although a straightforward solution is to collect more audio samples, we think this manner requires much time and effort and is not flexible.

To address the above issue of modality dominance, we propose a Modality Compensation Adapter (Figure 3b). Here, we only formalize the compensation for the audio modality below, and the same operation can be applied to the video counterpart.

$$c_t = e_t^a + \theta_c (Norm_{L2}(e_t^a), Norm_{L2}(e_t^v)) \quad (2)$$

where e_t^a , e_t^v are unimodal embeddings extracted by encoders and c_t denotes the compensated embeddings. Here we compensate audio modality by concatenating $L2$ normalization of each unimodal embedding and passing them through a learnable residual θ_c . We adopt audio compensation in our framework considering its contribution to balancing the two modalities and thus yielding more reasonable and preferable results that align with our speculation (as verified by the ablation study in Section V-E2).

3) **Dual-Label Classifier:** To achieve the goal of synergistic detection of both visual and auditory manipulation, we design a dual-label classifier that is composed of a Fake Composition Detector (FCD) and a Temporal Aggregation Module (TAM). This design is implemented based on two considerations. First, in the speech recognition architecture, it performs frame-wise prediction for each time step, whereby only frame-level outputs are served. However, for deepfake detection, frame-level output is insufficient to capture temporal jitter between consecutive frames. Straightforward conduction of a temporal-pooling operation might average these subtle clues, thus an interactive video-level information aggregation is needed to capture temporal inconsistency. Second, the real/fake discrepancy varies from different modalities. To bridge the forgery intensity gap across modalities and provide a generalizable representation, we impose an extra supervision from the given label to denote the forgery intensity, *i.e.*, the number of fake modalities in a given video. This practice is inspired by MITr [49], a successful work in multi-label classification because dual-label deepfake detection shares a similar concept with multi-label classification tasks in terms of the classification paradigm. In their work, they claim that this reinforced supervision can force the model to extract the common features of the same class and learn a more robust projection between features and labels, while our implementation aims at endowing a constraint of the same intensity to the audio or video manipulation in an explicit way. Specifically, despite their forgery intensity difference, in the case of only one modality has been manipulated in a certain video, whether it is visual, or audio, the intense label is assigned as 1. We believe that this design can provide a more generalizable representation, which is validated in the experiment section.

Based on the above consideration, we propose to implement these designs in our dual-label classifier via two transformer-like [50] modules. FCD serves for forgery intensity modeling and TAM for capturing temporal inconsistency. As shown in Figure 3c, leveraging the flexibility of transformer tokens, we

prepend two randomly initialized tokens at the head of the feature sequence: a fake-aware token \mathbf{T}_{fake} , and a temporal class token \mathbf{T}_{temp} , respectively. Formally, we redefine the compensated embeddings that have passed through the joint decoder as \hat{c}_t . The dimensions of the two tokens are the same as those of \hat{c}_t . We then proceed to perform dual-label classification as follows:

$$\mathbf{Seq}_{\text{temp}} = FCD(\text{Concat}(\mathbf{T}_{\text{fake}}; \hat{c}_1; \hat{c}_2 \dots \hat{c}_T)) \quad (3)$$

$$\mathbf{Seq} = TAM(\text{Concat}(\mathbf{T}_{\text{temp}}, \mathbf{Seq}_{\text{temp}})) \quad (4)$$

$$\tilde{y}_m^j = MLP(\mathbf{Seq}[0]), \tilde{p}^j = MLP(\mathbf{Seq}[1]) \quad (5)$$

where \mathbf{Seq} denotes the resultant output after FCD and TAM. $\mathbf{Seq}[0]$ and $\mathbf{Seq}[1]$ represent the corresponding outputs of the temporal class token \mathbf{T}_{temp} and the fake-aware token \mathbf{T}_{fake} , respectively, which are then processed by a multi-layer perceptron (MLP) to output the final predictions. The difference is that the temporal class token predicts specific forgery modalities \tilde{y}_m^j and is optimized by binary cross-entropy loss,

$$L_{bce} = \frac{1}{N_{df}} \sum_{j=1}^{N_{df}} \mathcal{L}_{\text{BCE}}(\tilde{y}_m^j, y_m^j; \theta_a, \theta_v, \theta_m, \theta_j, \theta_d) \quad (6)$$

while the fake-aware token outputs a prediction score for the number of fake modalities. Let \tilde{p}^j and p^j represent the prediction and ground truth of the fake-aware token, respectively. The ground truth is given by $p^j = \sum_{m \in \{a,v\}} y_m^j \in \{0, 1, 2\}$ to quantifies the number of fake modalities. The prediction is subsequently optimized using the cross-entropy loss,

$$L_{ce} = \frac{1}{N_{df}} \sum_{j=1}^{N_{df}} \mathcal{L}_{\text{CE}}(\tilde{p}^j, p^j; \theta_a, \theta_v, \theta_m, \theta_j, \theta_d) \quad (7)$$

Eventually, for the final framework, the overall learning objective can be defined as:

$$L = L_{bce} + L_{ce} \quad (8)$$

V. EXPERIMENTS AND RESULTS

A. Preprocessing

1) **Audio Stream:** The audio signals are all resampled at a 16kHz sample rate and applied Short Time Fourier Transform (STFT) to obtain 321-dimensional spectrograms, with a 40ms window and 10ms hop-length. Since the visual signals are sampled at 25 fps per video, each visual frame corresponds to 4 acoustic frames. Following AVSR, the acoustic frames are padded to make the input length a multiple of 4. Every 4 acoustic frames are concatenated and passed through a 1D convolutional layer with stride 4 to align input length with visual frames.

2) **Video Stream:** After sampling the video at 25fps, we perform face tracking using the S3FD face detector [51] for the video datasets that are not face-centered. For face-centered video frames, we resize it into a 224×224 and crop out a 112×112 patch that covers mouth region. Following Deep-AVSR, given a video of T frames, a spatio-temporal ResNet [52] is applied. After spatial average-pooling, a feature vector of $T \times 512$ is generated for each video.

B. Setup

1) **Implementation Details:** The overall framework is stacked by multiple transformer layers. The layer numbers of each module are specified in Table III.

TABLE III: The layer number of transformers in each module.

θ_a	θ_v	θ_j	θ_{d-FCD}	θ_{d-TAM}
6	6	6	1	2

The pretraining is based on the approach of DeepAVSR [43]. We select the TM-CTC model trained on LRS2 [53] dataset and use the publicly available, pretrained model.⁴ We adopt modality dropout during training, where dropout is applied to mask the full features of one modality, and the loss for the corresponding labels are also masked. We train the model with a batch size of 12 and Adam optimization [54] with a learning rate of 1e-5. Every model is trained for 100 iterations in total.

2) **Metrics:** The metric of our dual-label experiments is the F1 score. Since each dataset has varying degrees of class imbalances, we use average per-class F1 (CF1) and overall F1 (OF1). Actually, OF1 is preferable for class imbalance since it weighs each sample equally. To take the class size into consideration, we also report weighted-averaged F1 (WF1) scores which can account for the contribution of each class by weighting the number of samples of that given class. The accuracy score (ACC) is also used to evaluate the performance of each single modality detection. For comparative analysis with state-of-the-art methods, we adapt to the binary classification metrics employed in their studies.

C. Audio-Visual Deepfake Datasets

1) **DFDC:** DFDC [48] is a larger-scale dataset containing 128,154 videos, including 104,500 fake videos. Both audio manipulation and visual manipulation are involved in DFDC. Due to its large scale, previous works [8, 10, 11] did not perform experiments on the entire set of videos. A popular practice is to sample a subset from DFDC. Following prior works [8, 10], we sample the subset of 18,000 videos (85:15 train-test split) from DFDC. DFDC does not contain videos in which only the audio component is fake; only those videos with a manipulated visual component are further selected for audio swapping. Similar to [36], the specific fake audio label is given by comparing audio tracks of fake videos with those of original videos, which is achieved via hashing the audio file sequence.⁵

2) **FakeAVCeleb:** FakeAVCeleb [55] is a multimodal deepfake dataset tailored for audio-visual deepfake detection, consisting of 500 real videos and 19,500 deepfake videos. Its forgery types align more closely with our scenarios, as it includes deepfakes that are manipulated in audio-only, visual-only, and both audio-visual forms.

3) **LAV-DF:** Localized Audio Visual DeepFake (LAV-DF) [15] is a multimodal dataset in which local-manipulated contents exist in either the audio or video component (or both). It contains 136,304 videos, including 99,873 fake videos. Unlike the above two datasets, where fake content is throughout the entire video or audio signal, manipulation in LAV-DF is driven by transcript content. The word/words are replaced with their antonym(s) to generate small fake segments of audio or video.

D. Comparative Experiments

To demonstrate the effectiveness of our method, we conduct comparative experiments with state-of-the-art detectors on audio-visual, visual-only, and audio-only deepfakes, respectively.

1) **Audio-visual deepfake detection:** In this subsection, we first focus on a comparison with audio-visual deepfake detection methods. This means performing predictions at the entire video level, regardless of what the specific fake modality is. We report the AUC scores in Table IV. To ensure a fair comparison, particularly since different methods select various subsets on DFDC, we employ N-fold Cross-Validation across different subsets and report the mean AUC along with the standard deviation on it. As for FakeAVCeleb, we directly use full data following the splits for train/test from the original datasets. Notably, since the output of our method is the independent probability of each modality, we calculate the predicted authenticity of the entire video by multiplying the probability of the real class from each modality, which is then used to compute AUC scores.

TABLE IV: Comparison of **audio-visual** deepfake detection on DFDC and FakeAVCeleb datasets. Results of some methods are cited from AVoiD-DF [12] and PVASS [18].

Audio-Visual Methods	FakeAVCeleb		DFDC	
	ACC	AUC	ACC	AUC
MDS [8] (2020)	82.8	86.5	89.8	91.6
EmoForen [10] (2020)	78.1	79.8	80.6	84.4
AVFakeNet [16] (2022)	78.4	83.4	82.8	86.2
VFD [13] (2022)	81.5	86.1	80.9	85.1
BA-TFD [15] (2022)	80.8	84.9	79.1	84.6
JointAV [11] (2021)	82.5	83.3	90.2	91.9
AVoiD-DF [12] (2023)	83.7	89.2	91.4	94.8
AVAD [17] (2023)	94.2	94.5	93.2	96.7
PVASS [18] (2023)	95.7	97.3	96.3	98.9
Ours	99.7	99.9	91.2±0.3	96.9±0.4

Table IV shows that our framework outperforms all other methods on the FakeAVCeleb dataset and yields competitive results on DFDC. For DFDC, our AUC scores are comparable to very recent methods like PVASS, although our ACC scores are lower. This is because ACC is a metric that is more sensitive to class imbalance. The audio deepfakes are far fewer than visual deepfakes in DFDC, which makes our framework prone to lower scores when calculating overall video-level accuracy. Unlike DFDC, which is predominantly composed of face-swapped videos, FakeAVCeleb introduces more complex cross-modal forgery patterns by incorporating deepfakes generated by Wav2lip. Specifically, the audio content drives the lip movements, creating a unique type of forgery. Our method

⁴https://github.com/lordmartian/deep_avsr

⁵<https://www.kaggle.com/datasets/basharallabadi/dfdc-video-audio-labels>

is particularly well-suited to combat these kinds of forgeries by effectively modeling cross-modal speech correlations. In contrast, methods like EmoForen, which rely on emotion correlation across modalities, fall short in their effectiveness. Our approach, focusing on speech correlation, proves to be more effective in detecting these sophisticated forgeries.

TABLE V: Comparison on local-manipulated audio-visual deepfakes using AUC metrics. Results of other methods are cited from LAV-DF [15].

LAV-DF			
MDS [8] (2020)	EffiViT [56] (2022)	BA-TFD [15] (2022)	Ours
82.8	96.5	99.0	99.9

In addition to traditional deepfake datasets, we also evaluate the performance of our methods on partially modified deepfakes on LAV-DF. These subtle fake contents are more indistinguishable and imperceptible due to their lesser discrepancy from real content. Detecting this type of localized forgery could be more valuable and challenging in practical application scenarios. As shown in Table V, the results on LAV-DF show that our method also outperforms the other compared methods which demonstrates our methods can also combat such novelty deepfakes well.

2) *Visual-only deepfake detection*: In this subsection, we report the performance of binary prediction for visual deepfake detection and compare it with state-of-the-art video-only detection methods. This means our framework is fed only with the video stream as input during the test, corresponding to the scenarios of missing audio modality.

TABLE VI: Comparison of **visual-only** deepfake detection on DFDC and FakeAVCeleb datasets.

Visual-Only Methods	FakeAVCeleb		DFDC	
	ACC	AUC	ACC	AUC
MesoNet [57] (2018)	57.3	60.9	71.7	75.3
Capsule [58] (2019)	68.8	70.9	50.2	53.3
HeadPose [59] (2019)	45.6	49.2	51.4	55.9
VA-MLP [60] (2019)	65.0	67.1	59.3	61.9
Xception [61] (2019)	67.9	70.5	46.5	49.9
LipForensics [30] (2021)	80.1	82.4	71.3	73.5
DeFakeHop [62] (2021)	68.3	71.6	78.9	81.1
CViT [63] (2021)	69.7	71.8	62.1	63.7
MaDD [23] (2021)	77.6	79.3	82.5	84.8
SLADD [64] (2022)	70.5	72.1	73.6	75.2
RealForensics [14] (2022)	90.1	92.3	89.6	91.5
Ours (Video Only)	99.6	99.9	89.3 ± 0.7	96.7 ± 0.4

As shown in Table VI, our framework achieves the best performance on both datasets. Our framework outperforms advanced self-supervised methods like SLADD and RealForensics. RealForensics employs audio in its self-supervised training to learn a natural cross-modal representation. We include its results here due to its visual-only settings at test time. Although it achieves competitive results, it leaves high-level semantic features underutilized, placing its performance behind ours. LipForensics emphasizes the effectiveness of high-level semantic information via clip-wise lipreading, which differs from our frame-wise phoneme prediction approach, resulting in their limited performance. We attribute our superior performance to the leveraging of frame-wise phoneme

speech features, which is beneficial in capturing more fine-grained forgery clues.

3) *Audio-only deepfake detection*: In this subsection, we report the performance of binary prediction for audio deepfake detection and compare it with works specifically dedicated to combating audio-only deepfakes. For these experiments, we exclusively feed the audio stream into our framework to align with the scenarios of missing visual modality. Given that DFDC is primarily utilized for visual deepfake detection in current literature, here we only report the performance on FakeAVCeleb. Following their conventions, we use EER (Equal Error Rate) and the AUC score as evaluation metrics. We choose to benchmark against the work presented in DAD-SV [35], which detects audio deepfakes via the Speaker Verification task. This is because both our methods and DAD-SV share a similar strategy: leveraging external pre-tasks to extract high-level information beneficial for deepfake detection. The key difference is that DAD-SV compares the audio to be detected with pristine audio from the same individual to determine authenticity, requiring them to rely on pre-acquired identity information of the test audio. In contrast, our method focuses more on semantic information for detection.

TABLE VII: Comparison of **audio-only** deepfake detection on FakeAVCeleb dataset.

Audio-Only Methods	EER	AUC
LCNN-LSTM-sum-p2s [65]	0.39	67.3
RawGATstMul [66]	0.66	30.5
RawNet2 [67]	0.55	45.5
ClovaAI [68]	0.40	62.8
H/ASP [69]	0.14	93.5
ECAPA-TDNN [70]	0.21	86.2
POI-Forensics [71]	0.21	85.8
POI-Forensics + aug [71]	0.26	82.4
Ours (Audio Only)	0.01	99.9

As shown in Table VII, we compare our results with supervised learning baseline models [65–67] and the speaker verification based methods [68–71] that DAD-SV employed in their works. Our method demonstrates superior performance, surpassing all baseline methods as well as the best-performing speaker verification method, H/ASP, by more than 6% on AUC. The results also indicate that both speaker verification methods and our method generally outperform supervised methods. This suggests that the incorporation of external prior information can indeed benefit deepfake detection. Nevertheless, methods that rely on identity information may be constricted by the specific identity in the reference dataset. Our approach focuses more on semantic aspects, allowing our method to achieve further improvement.

E. Ablation Study

1) *Benefit of AVSR*: To demonstrate the effectiveness of audio-visual speech correlation for dual-label deepfake detection, we train a framework the same as our final framework from scratch without AVSR weights loaded for comparison.

As shown in Table VIII, introducing the AVSR task significantly improves the detection performance, which verifies that potential speech correlation across modalities is highly

TABLE VIII: Benefit of AVSR.

Dataset	DFDC			LAV-DF			FakeAVCeleb		
Method	OF1	CF1	WF1	OF1	CF1	WF1	OF1	CF1	WF1
w/o AVSR	77.52	75.60	76.78	95.65	95.66	95.53	98.95	99.04	98.70
w/ AVSR	90.24	87.80	90.24	99.85	99.85	99.86	99.87	99.89	99.89

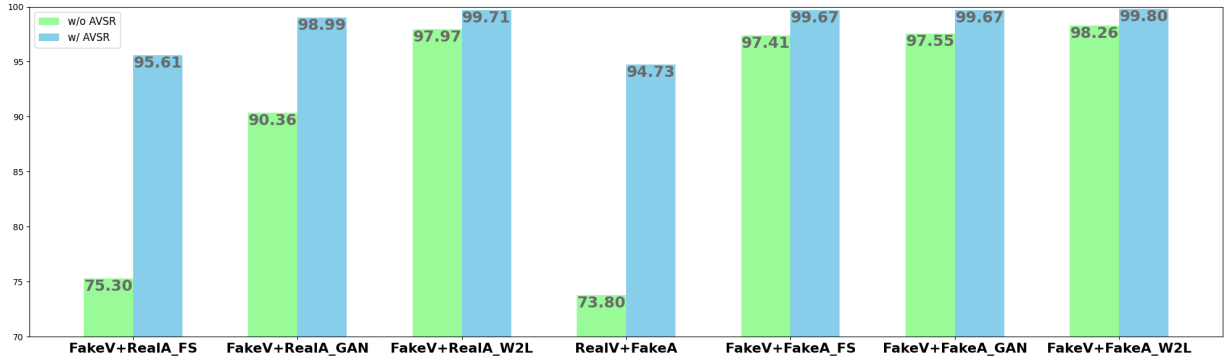


Fig. 4: The performance comparison on different types of fake videos on the FakeAVCeleb dataset.

beneficial to synergistic audio-visual deepfake detection. The improvement is not only reflected in globally forged DFDC and FakeAVCeleb but also in locally forged LAV-DF. Albeit LAV-DF proves that changing a few uttering words can even lead to a subtle forgery beyond the perception of humans, leveraging AVSR allows us to extract phoneme-level features frame by frame. The promising potential of these fine-grained semantic features will show more value in real-life scenarios.

The extent of speech correlation might not be uniform and varies based on the specific deepfake generation method employed. To further investigate the impact of potential speech correlation across various deepfake categories, we examine the performance of each fake type on the FakeAVCeleb dataset. As shown in Figure 4, we present a comparative analysis based on the OF1 score for each type, both with and without the incorporation of audio-visual speech recognition. Here we append a suffix behind the forgery type of each modality to denote the manipulated methods, resulting a seven categories, including (1)“FakeV+RealA_FS”: real audio with fake video by FaceSwap; (2) “FakeV+RealA_GAN”: real audio with fake video by FSGAN; (3)“FakeV+RealA_W2L”: real audio with fake video by Wav2Lip; (4) “RealV+FakeA”: real video with fake audio by SV2TTS; (5) “FakeV+FakeA_FS”: fake video by FaceSwap and Wav2Lip, and fake audio by SV2TTS; (6) “FakeV+FakeA_GAN”: fake video by FSGAN and Wav2Lip, and fake audio by SV2TTS; (7) “FakeV+FakeA_Ori”: fake video by Wav2Lip, and fake audio by SV2TTS. As all types with fake audio are generated by SV2TTS, here we omit it in the suffix. Notably, “FakeV+FakeA_Ori” denotes that the fake video content is created solely through the lip-syncing process via Wav2lip, which drives the fake audio to generate lip movements on the original face. Here, we use “Ori” to denote the absence of any extra face-swapping process.

As illustrated in Figure 4, our method consistently performs well across all types of forgeries. It shows an especially significant improvement in the “RealV+FakeA” category. This is because the fake audio in this case is generated by the

text-driving method and fails to reproduce natural temporal synchronization with the lip movements of the original video. Yet, our method is particularly adept at capturing this audio-visual asynchrony. Moreover, our method surpasses 99% on all forgery types generated by Wav2Lip, which re-proves our strength in capturing cross-modal fake clues.

2) **Benefit of modality compensation:** In this section, we evaluate how the form of the modality compensation strategy affects the performance of dual-label deepfake detection on DFDC. We evaluate the variants of (1) the simple concatenation of two modalities with no compensation (**None**), as preceding speech recognition does; (2) audio modality compensated (**Audio**); (3) video modality compensated (**Video**). We also show the detection performance of each single modality (**AF1** for audio, and **VF1** for video). As shown in Table IX,

TABLE IX: Ablation results of different strategies of modality compensation.

Compensation	OF1	CF1	VF1	AF1	WF1
None	88.96	86.02	89.62	82.40	88.57
Video	87.79	84.41	88.50	80.17	87.57
Audio	90.24	87.80	90.84	84.61	90.24

consistent with our speculation in section IV-B2, adopting audio modality compensation yields the most desirable performance. Notably, compared with video compensation, audio compensation improves not only audio detection performance but also that of video. Since the influence of audio on model decision-making tends to be weaker, we believe a balance between audio and visual modalities is achieved by this mechanism and helps both modalities learn better features.

3) **Generalization ability of sub-modules in dual-label classifier:** We expect the design of TAM and FCD in the Dual-Label Classifier to provide a more generalizable audio-visual representation. Here, we develop two variants and conduct a series of experiments of cross-dataset tests to investigate the influence of different components. We train our framework on

TABLE X: Generalization study on the influence of different components in Dual-Label Classifier. The CrossFakeAVCeleb denotes trained on DFDC and tested on FakeAVCeleb, and vice versa.

Methods	CrossFakeAVCeleb					CrossDFDC				
	OF1	CF1	WF1	VACC	AACC	OF1	CF1	WF1	VACC	AACC
w/o TAM&FCD	65.77	54.07	57.12	74.73	49.34	55.89	29.23	53.00	58.46	94.65
w/o TAM	67.50	55.53	59.68	76.41	49.55	58.28	32.67	55.77	59.19	94.61
Ours	68.57	55.83	58.77	80.00	48.89	58.57	36.97	56.75	61.42	94.07

TABLE XI: Comparison of our dual-label framework with unimodal approaches and multi-classifier approaches under three test modality-agnostic cases: prediction with visual-only (shown in pink), audio-only (shown in green), or audio-visual input. The best results are highlighted in bold.

Available Modality		Classification	FakeAVCeleb				DFDC			
Audio	Visual	Type	VACC	AACC	VF1	AF1	VACC	AACC	VF1	AF1
√	-	Binary	-	96.99	-	97.23	-	75.79	-	68.04
-	√	Binary	89.59	-	98.96	-	84.19	-	84.61	-
√	-	Dual-classifier	-	97.16	-	97.35	-	97.54	-	66.67
-	√	Dual-classifier	99.50	-	99.74	-	87.96	-	87.95	-
√	√	Dual-classifier	99.64	99.88	99.81	99.88	90.07	98.34	89.33	83.14
√	-	Triple-classifier	-	98.19	-	98.24	-	95.80	-	59.77
-	√	Triple-classifier	99.48	-	99.72	-	87.58	-	87.97	-
√	√	Triple-classifier	99.64	99.95	99.81	99.95	89.96	98.15	89.21	82.22
√	-	Dual-Label	-	99.95	-	99.95	-	98.27	-	81.33
-	√	Dual-Label	99.65	-	99.81	-	90.50	-	89.96	-
√	√	Dual-Label	99.70	99.93	99.84	99.93	91.23	98.46	90.83	84.61

both FakeAVCeleb and DFDC and mutually perform cross-dataset tests.

As shown in Table X, the general results indicate that the absence of the TAM leads to a decline in generalization performance on both datasets. Moreover, the deletion of the FCD further exacerbates this decline, which verifies the importance of bridging the forgery intensity gap across modalities. Overall, performance on both datasets reaches its peak when all components are employed in the Dual-Label Classifier.

4) *Benefit of dual-label classifier*: To investigate the impact of dual-label manner on the detection of each modality, we adapt our framework into various variants based on the involved modality and classification approach. First, we trained two separate unimodal models for audio and video modalities to serve as baselines. Additionally, we adapted our framework to align with previous multimodal approaches, transforming it into two variants of multi-classifier methods: a dual-classifier (i.e., for audio and visual streams, respectively) as done in AVFakeNet, and a triple-classifier (i.e., for audio, visual, and entire video, respectively) as implemented in JointAV. As presented in Table XI, these comparative experiments, along with our proposed method, constitute three groups of experiments. Under each group of experiments, we report three types of test results to examine the performance under modality-agnostic scenarios, i.e., after training is completed in a multimodal setting, the model performs prediction with visual-only (shown in pink), audio-only (shown in green), or audio-visual input during the testing phase.

It can be observed that no matter whether compared to unimodal approaches or classifier variants, our method performs best on all metrics for both datasets, particularly in cases where both audio and video are available. In fact, with the support of AVSR, under such a test case that is consistent with training conditions, the results produced by different classifier variants

exhibit minor differences and all surpass unimodal methods. This highlights the advantage of AVSR in modeling cross-modal forgery clues when compared to unimodal methods.

In more challenging missing modality situations, our method further extends its lead over other variants by maintaining performance on par with audio-visual detection. When either modality is unavailable, the variation in our method’s performance on the FakeAVCeleb dataset remains minimal, within decimal point ranges. However, both dual and triple classifiers experience a decline of over 1 percentage point in the audio-only input situation. This gap is more evident in DFDC which is dominated by visual forgeries, where both the AF1 for dual classifiers and triple classifiers exhibit a more significant decline. For video-only detection, our method continues to outperform the unimodal baseline and other variants. The combined results from both datasets show that our method consistently maintains its advantages over unimodal approaches in their respective modalities, regardless of whether the modalities are present in pairs or not.

We attribute the effectiveness of our method to the fact that, compared to multiple classifiers that create a branched structure, the dual-label approach results in a highly-multiplexed unified structure that more effectively preserves the forgery patterns extracted by AVSR. In essence, the dual-label technique optimizes the benefits of AVSR. Overall, the performance on audio-only, visual-only, and audio-visual detection collectively demonstrates that the proposed framework excels in all three fake-modality-agnostic scenarios.

F. Visualization

To demonstrate the efficacy of each design, we visualize the feature cluster of four categories with regard to manipulated modalities, namely, “RealV+RealA”, “RealV+FakeA”, “FakeV+RealA”, and “FakeV+FakeA”. We employ t-SNE

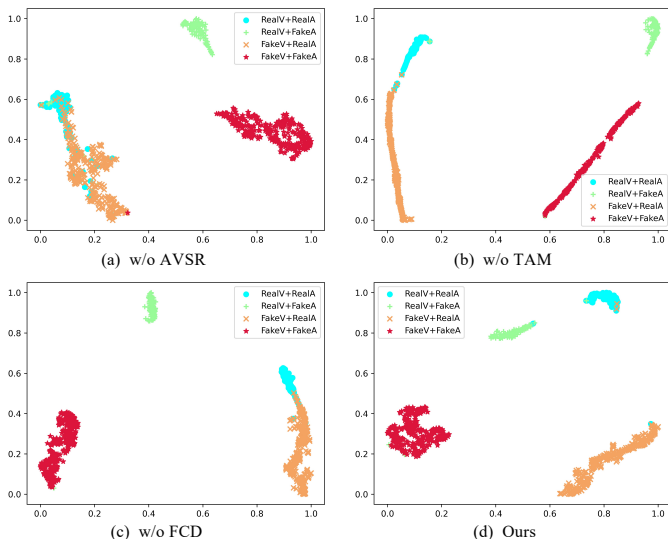


Fig. 5: T-SNE visualization of feature space learned by variants of our framework.

[72] to visualize the feature distribution of the test set from FakeAVCeleb. As shown in Figure 5, without finetuning on AVSR (Figure a), the model suffers from the most severe feature entanglement. After finetuning on AVSR (Figure b, c, d), the features exhibit better distinguishability. However, the absence of either TAM or FCD still leaves the distinguishability of video-only fakes (orange) not satisfactory enough. Collectively, our framework generates the most favorable feature distribution. As depicted in Figure 5d, the distributions of four categories are disentangled well. Notably, among the three fake distributions, the feature clusters of audio-only fakes (green) and video-only fakes (orange) are relatively close to that of the reals (blue), and the audio-visual fakes (red) are most distant from the reals as they possess more fake compositions, which is consistent with our description of forgery intensity. We believe this optimal feature distribution also reflects the contribution of FCD.

VI. CONCLUSION

This paper presents a unified, modality-agnostic framework capable of detecting audio-visual deepfakes, regardless of the number or type of modality involved. We designed a dual-label detection classifier to specifically identify whether either the audio or visual modality (or both) has been manipulated, while effectively handling scenarios with missing modalities. The AVSR is introduced to provide high-level speech correlations across modalities, enhancing the framework’s ability to model cross-modal forgery clues. The integration of AVSR with the Dual-Label Classifier results in excellent performance for each individual modality. The overall component design leads our framework to not only outperform various state-of-the-art competitors but also effectively detect modality-agnostic audio-visual deepfakes with promising performance. In our future work, we will expand our investigation to cover a broader spectrum of multimodal forgery types and enhance the performance for complex talking scenarios.

REFERENCES

- [1] I. Korshunova, W. Shi, J. Dambre, and L. Theis, “Fast face-swap using convolutional neural networks,” in *Proceedings of the IEEE international conference on computer vision*, 2017, pp. 3677–3685.
- [2] J. Thies, M. Zollhofer, M. Stamminger, C. Theobalt, and M. Nießner, “Face2face: Real-time face capture and reenactment of rgb videos,” in *Proceedings of the IEEE conference on computer vision and pattern recognition*, 2016, pp. 2387–2395.
- [3] A. Siarohin, S. Lathuilière, S. Tulyakov, E. Ricci, and N. Sebe, “First order motion model for image animation,” *Advances in Neural Information Processing Systems*, vol. 32, 2019.
- [4] W. Ping, K. Peng, and J. Chen, “Clarinet: Parallel wave generation in end-to-end text-to-speech,” *arXiv preprint arXiv:1807.07281*, 2018.
- [5] H. Kameoka, T. Kaneko, K. Tanaka, and N. S.-V. Hojo, “Non-parallel many-to-many voice conversion using star generative adversarial networks,” in *SLT Workshop*, 2018, pp. 18–21.
- [6] K. Prajwal, R. Mukhopadhyay, V. P. Namboodiri, and C. Jawahar, “A lip sync expert is all you need for speech to lip generation in the wild,” in *MM*, 2020, pp. 484–492.
- [7] K. Cheng, X. Cun, Y. Zhang, M. Xia, F. Yin, M. Zhu, X. Wang, J. Wang, and N. Wang, “Videoretalking: Audio-based lip synchronization for talking head video editing in the wild,” 2022.
- [8] K. Chugh, P. Gupta, A. Dhall, and R. Subramanian, “Not made for each other-audio-visual dissonance-based deepfake detection and localization,” in *MM*, 2020, pp. 439–447.
- [9] Y. Gu, X. Zhao, C. Gong, and X. Yi, “Deepfake video detection using audio-visual consistency,” in *International Workshop on Digital Watermarking*. Springer, 2020, pp. 168–180.
- [10] T. Mittal, U. Bhattacharya, R. Chandra, A. Bera, and D. Manocha, “Emotions don’t lie: An audio-visual deepfake detection method using affective cues,” in *MM*, 2020, pp. 2823–2832.
- [11] Y. Zhou and S.-N. Lim, “Joint audio-visual deepfake detection,” in *ICCV*, 2021, pp. 14 800–14 809.
- [12] W. Yang, X. Zhou, Z. Chen, B. Guo, Z. Ba, Z. Xia, X. Cao, and K. Ren, “Avoid-df: Audio-visual joint learning for detecting deepfake,” *IEEE Transactions on Information Forensics and Security*, vol. 18, pp. 2015–2029, 2023.
- [13] H. Cheng, Y. Guo, T. Wang, Q. Li, T. Ye, and L. Nie, “Voice-face homogeneity tells deepfake,” *arXiv preprint arXiv:2203.02195*, 2022.
- [14] A. Haliassos, R. Mira, S. Petridis, and M. Pantic, “Leveraging real talking faces via self-supervision for robust forgery detection,” in *CVPR*, 2022, pp. 14 950–14 962.
- [15] Z. Cai, K. Stefanov, A. Dhall, and M. Hayat, “Do you really mean that? content driven audio-visual deepfake dataset and multimodal method for temporal forgery localization,” *arXiv preprint arXiv:2204.06228*, 2022.

- [16] H. Ilyas, A. Javed, and K. M. Malik, “Avfakenet: A unified end-to-end dense swin transformer deep learning model for audio–visual deepfakes detection,” *Applied Soft Computing*, vol. 136, p. 110124, 2023.
- [17] C. Feng, Z. Chen, and A. Owens, “Self-supervised video forensics by audio-visual anomaly detection,” *arXiv preprint arXiv:2301.01767*, 2023.
- [18] Y. Yu, X. Liu, R. Ni, S. Yang, Y. Zhao, and A. C. Kot, “Pvass-mdd: Predictive visual-audio alignment self-supervision for multimodal deepfake detection,” *IEEE Transactions on Circuits and Systems for Video Technology*, 2023.
- [19] L. Li, J. Bao, T. Zhang, H. Yang, D. Chen, F. Wen, and B. Guo, “Face x-ray for more general face forgery detection,” in *CVPR*, 2020, pp. 5001–5010.
- [20] K. Shiohara and T. Yamasaki, “Detecting deepfakes with self-blended images,” in *CVPR*, 2022, pp. 18 720–18 729.
- [21] Q. Gu, S. Chen, T. Yao, Y. Chen, S. Ding, and R. Yi, “Exploiting fine-grained face forgery clues via progressive enhancement learning,” in *AAAI*, vol. 36, no. 1, 2022, pp. 735–743.
- [22] C. Yu, P. Chen, J. Dai, X. Wang, W. Zhang, J. Liu, and J. Han, “Focus by prior: Deepfake detection based on prior-attention,” in *2022 IEEE International Conference on Multimedia and Expo (ICME)*. IEEE, 2022, pp. 1–6.
- [23] H. Zhao, W. Zhou, D. Chen, T. Wei, W. Zhang, and N. Yu, “Multi-attentional deepfake detection,” in *CVPR*, 2021, pp. 2185–2194.
- [24] S. Agarwal, H. Farid, Y. Gu, M. He, K. Nagano, and H. Li, “Protecting world leaders against deep fakes,” in *CVPR Workshops*, vol. 1, 2019, p. 38.
- [25] Z. Sun, Y. Han, Z. Hua, N. Ruan, and W. Jia, “Improving the efficiency and robustness of deepfakes detection through precise geometric features,” in *CVPR*, 2021, pp. 3609–3618.
- [26] Y. Li, M.-C. Chang, and S. Lyu, “In ictu oculi: Exposing ai created fake videos by detecting eye blinking,” in *WIFS*. IEEE, 2018, pp. 1–7.
- [27] Z. Gu, Y. Chen, T. Yao, S. Ding, J. Li, and L. Ma, “Delving into the local: Dynamic inconsistency learning for deepfake video detection,” in *AAAI*. AAAI Press, 2022, pp. 744–752. [Online]. Available: <https://ojs.aaai.org/index.php/AAAI/article/view/19955>
- [28] D. Zhang, C. Li, F. Lin, D. Zeng, and S. Ge, “Detecting deepfake videos with temporal dropout 3dcnn,” in *IJCAI*, 2021, pp. 1288–1294.
- [29] Z. Gu, Y. Chen, T. Yao, S. Ding, J. Li, F. Huang, and L. Ma, “Spatiotemporal inconsistency learning for deepfake video detection,” in *CVPR*, 2021, pp. 3473–3481.
- [30] A. Haliassos, K. Vougioukas, S. Petridis, and M. Pantic, “Lips don’t lie: A generalisable and robust approach to face forgery detection,” in *CVPR*, 2021, pp. 5039–5049.
- [31] J. M. Martín-Doñas and A. Álvarez, “The vicomtech audio deepfake detection system based on wav2vec2 for the 2022 add challenge,” in *ICASSP*. IEEE, 2022, pp. 9241–9245.
- [32] Y. Xie, Z. Zhang, and Y. Yang, “Siamese network with wav2vec feature for spoofing speech detection,” in *Inter-speech*, 2021, pp. 4269–4273.
- [33] X. Wang and J. Yamagishi, “Investigating self-supervised front ends for speech spoofing countermeasures,” *arXiv preprint arXiv:2111.07725*, 2021.
- [34] A. Baevski, Y. Zhou, A. Mohamed, and M. Auli, “wav2vec 2.0: A framework for self-supervised learning of speech representations,” *NeurIPS*, vol. 33, pp. 12 449–12 460, 2020.
- [35] A. Pianese, D. Cozzolino, G. Poggi, and L. Verdoliva, “Deepfake audio detection by speaker verification,” in *2022 IEEE International Workshop on Information Forensics and Security (WIFS)*. IEEE, 2022, pp. 1–6.
- [36] B. Hosler, D. Salvi, A. Murray, F. Antonacci, P. Bestagini, S. Tubaro, and M. C. Stamm, “Do deepfakes feel emotions? a semantic approach to detecting deepfakes via emotional inconsistencies,” in *CVPR*, 2021, pp. 1013–1022.
- [37] B. Shi, W.-N. Hsu, K. Lakhotia, and A. Mohamed, “Learning audio-visual speech representation by masked multimodal cluster prediction,” in *ICLR*, 2021.
- [38] R. Campbell, “The processing of audio-visual speech: empirical and neural bases,” *Philosophical Transactions of the Royal Society B: Biological Sciences*, vol. 363, no. 1493, pp. 1001–1010, 2008.
- [39] I. Almajai and B. Milner, “Maximising audio-visual speech correlation,” in *AVSP*, 2007, p. 17.
- [40] S. Agarwal, H. Farid, O. Fried, and M. Agrawala, “Detecting deep-fake videos from phoneme-viseme mismatches,” in *CVPR Workshops*, 2020, pp. 2814–2822.
- [41] M. Ma, J. Ren, L. Zhao, S. Tulyakov, C. Wu, and X. Peng, “Smil: Multimodal learning with severely missing modality,” in *Proceedings of the AAAI Conference on Artificial Intelligence*, vol. 35, no. 3, 2021, pp. 2302–2310.
- [42] S. Petridis, Z. Li, and M. Pantic, “End-to-end visual speech recognition with lstms,” in *2017 IEEE International Conference on Acoustics, Speech and Signal Processing (ICASSP)*, 2017, pp. 2592–2596.
- [43] T. Afouras, J. S. Chung, A. Senior, O. Vinyals, and A. Zisserman, “Deep audio-visual speech recognition,” *TPAMI*, 2018.
- [44] S. Zhang, M. Lei, B. Ma, and L. Xie, “Robust audio-visual speech recognition using bimodal dfsmn with multi-condition training and dropout regularization,” in *ICASSP 2019 - 2019 IEEE International Conference on Acoustics, Speech and Signal Processing (ICASSP)*, 2019, pp. 6570–6574.
- [45] T. Makino, H. Liao, Y. Assael, B. Shillingford, B. Garcia, O. Braga, and O. Siohan, “Recurrent neural network transducer for audio-visual speech recognition,” in *2019 IEEE Automatic Speech Recognition and Understanding Workshop (ASRU)*, 2019, pp. 905–912.
- [46] A. Graves, S. Fernández, F. Gomez, and J. Schmidhuber, “Connectionist temporal classification: labelling unsegmented sequence data with recurrent neural networks,” in *ICML*, 2006, pp. 369–376.
- [47] P. Ma, S. Petridis, and M. Pantic, “End-to-end audio-

- visual speech recognition with conformers,” in *ICASSP*. IEEE, 2021, pp. 7613–7617.
- [48] B. Dolhansky, R. Howes, B. Pflaum, N. Baram, and C. C. Ferrer, “The deepfake detection challenge (dfdc) preview dataset,” *arXiv preprint arXiv:1910.08854*, 2019.
- [49] X. Cheng, H. Lin, X. Wu, F. Yang, D. Shen, Z. Wang, N. Shi, and H. Liu, “Mltr: Multi-label classification with transformer,” *arXiv preprint arXiv:2106.06195*, 2021.
- [50] A. Vaswani, N. Shazeer, N. Parmar, J. Uszkoreit, L. Jones, A. N. Gomez, Ł. Kaiser, and I. Polosukhin, “Attention is all you need,” in *NeurIPS*, 2017, pp. 5998–6008.
- [51] S. Zhang, X. Zhu, Z. Lei, H. Shi, X. Wang, and S. Z. Li, “S3fd: Single shot scale-invariant face detector,” in *ICCV*, 2017, pp. 192–201.
- [52] T. Stafylakis and G. Tzimiropoulos, “Combining residual networks with lstms for lipreading,” *Interspeech*, pp. 3652–3656, 2017.
- [53] J. Son Chung, A. Senior, O. Vinyals, and A. Zisserman, “Lip reading sentences in the wild,” in *Proceedings of the IEEE conference on computer vision and pattern recognition*, 2017, pp. 6447–6456.
- [54] D. P. Kingma and J. Ba, “Adam: A method for stochastic optimization,” *arXiv preprint arXiv:1412.6980*, 2014.
- [55] H. Khalid, S. Tariq, M. Kim, and S. S. Woo, “FakeAVCeleb: A novel audio-video multimodal deepfake dataset,” in *NeurIPS*, 2021. [Online]. Available: <https://openreview.net/forum?id=TAXFsg6ZaOl>
- [56] D. A. Coccomini, N. Messina, C. Gennaro, and F. Falchi, “Combining efficientnet and vision transformers for video deepfake detection,” in *International Conference on Image Analysis and Processing*. Springer, 2022, pp. 219–229.
- [57] D. Afchar, V. Nozick, J. Yamagishi, and I. Echizen, “Mesonet: a compact facial video forgery detection network,” in *WIFS*. IEEE, 2018, pp. 1–7.
- [58] H. H. Nguyen, J. Yamagishi, and I. Echizen, “Capsule-forensics: Using capsule networks to detect forged images and videos,” in *ICASSP*. IEEE, 2019, pp. 2307–2311.
- [59] X. Yang, Y. Li, and S. Lyu, “Exposing deep fakes using inconsistent head poses,” in *ICASSP*. IEEE, 2019, pp. 8261–8265.
- [60] F. Matern, C. Riess, and M. Stamminger, “Exploiting visual artifacts to expose deepfakes and face manipulations,” in *WACV Workshops*, 2019, pp. 83–92.
- [61] A. Rossler, D. Cozzolino, L. Verdoliva, C. Riess, J. Thies, and M. Nießner, “Faceforensics++: Learning to detect manipulated facial images,” in *ICCV*, 2019, pp. 1–11.
- [62] H.-S. Chen, M. Rouhsedaghat, H. Ghani, S. Hu, S. You, and C.-C. J. Kuo, “Defakehop: A light-weight high-performance deepfake detector,” in *2021 IEEE International conference on Multimedia and Expo (ICME)*. IEEE, 2021, pp. 1–6.
- [63] D. Wodajo and S. Atnafu, “Deepfake video detection using convolutional vision transformer,” *arXiv preprint arXiv:2102.11126*, 2021.
- [64] L. Chen, Y. Zhang, Y. Song, L. Liu, and J. Wang, “Self-supervised learning of adversarial example: Towards good generalizations for deepfake detection,” in *Proceedings of the IEEE/CVF Conference on Computer Vision and Pattern Recognition (CVPR)*, June 2022, pp. 18 710–18 719.
- [65] X. Wang and J. Yamagishi, “A comparative study on recent neural spoofing countermeasures for synthetic speech detection,” in *Interspeech*, 2021, pp. 4259–4263.
- [66] H. Tak, J.-w. Jung, J. Patino, M. Kamble, M. Todisco, and N. Evans, “End-to-end spectro-temporal graph attention networks for speaker verification anti-spoofing and speech deepfake detection,” *Automatic Speaker Verification and Spoofing Countermeasures Challenge*, 2021.
- [67] H. Tak, J. Patino, M. Todisco, A. Nautsch, N. Evans, and A. Larcher, “End-to-end anti-spoofing with rawnet2,” in *ICASSP 2021-2021 IEEE International Conference on Acoustics, Speech and Signal Processing (ICASSP)*. IEEE, 2021, pp. 6369–6373.
- [68] J. S. Chung, J. Huh, S. Mun, M. Lee, H.-S. Heo, S. Choe, C. Ham, S.-Y. Jung, B.-J. Lee, and I. Han, “In defence of metric learning for speaker recognition,” in *Interspeech*, 2020, pp. 2977–2981.
- [69] H. S. Heo, B.-J. Lee, J. Huh, and J. S. Chung, “Clova baseline system for the voxceleb speaker recognition challenge 2020,” *arXiv preprint arXiv:2009.14153*, 2020.
- [70] B. Desplanques, J. Thienpondt, and K. Demuynck, “Ecapa-tdnn: Emphasized channel attention, propagation and aggregation in tdnn based speaker verification,” pp. 3830–3834, 2020.
- [71] D. Cozzolino, A. Pianese, M. Nießner, and L. Verdoliva, “Audio-visual person-of-interest deepfake detection,” in *Proceedings of the IEEE/CVF Conference on Computer Vision and Pattern Recognition (CVPR) Workshops*, June 2023, pp. 943–952.
- [72] L. Van der Maaten and G. Hinton, “Visualizing data using t-sne.” *Journal of machine learning research*, vol. 9, no. 11, 2008.